THE ASTROPHYSICAL JOURNAL, 319:456–464, 1987 August 1

18 CENTIMETER VLBI OBSERVATIONS OF THE QUASAR NRAO 140 DURING AND AFTER A LOW-FREQUENCY OUTBURST

ALAN P. MARSCHER
Department of Astronomy, Boston University
JOHN J. BRODERICK
Department of Physics, Virginia Polytechnic Institute and State University
LUCIA PADRIELLI
Instituto di Radioastronomia, Bologna
NORBERT BARTEL
Harvard-Smithsonian Center for Astrophysics
AND
JONATHAN D. ROMNEY
National Radio Astronomy Observatory[1]
Received 1986 November 26; accepted 1987 January 26

ABSTRACT

We have observed the quasar NRAO 140 using an eight station very long baseline array at 18 cm in 1984 April and a seven station array at 6 cm in 1984 May. We compare both the map and the data at 18 cm with those obtained by Marscher and Broderick in 1981 October. The latter coincided with a $\sim 25\%$ outburst in flux density at wavelengths greater than ~ 30 cm. The differences in the maps are difficult to analyze directly owing to a blending at 18 cm of the components resolved at 6 cm. The minima in the 18 cm visibilities on the longest baselines, however, show significant shifts between epochs. Analysis of these shifts, using the 6 cm map and the overall spectrum as guides, indicates that a component ~ 5 milli-arc seconds southeast of the "core" dropped significantly in brightness between 1981 October, the epoch at which the total flux density at $\lambda > 30$ cm peaked, and 1984 April. We identify this component as the likely site of the low-frequency variations.

We compare the properties of low-frequency variability in NRAO 140 with the predictions of several models. The refractive scintillation model alone does not account for the source's properties. At least one additional feature (relativistic motion or high brightness temperature emission mechanisms) must be added in order to avoid excessive total energy requirements.

Subject headings: quasars — interferometry

I. INTRODUCTION

The phenomenon of low-frequency ($\lesssim 1$ GHz) variability on time scales of months or years in extragalactic radio sources (Hunstead 1972; see also Altschuler *et al.* 1984 and references therein) places severe constraints on the emission mechanism, source geometry, or velocity of the emitting region (cf., e.g., Jones and Burbidge 1973; Cotton and Spangler 1982). These constraints arise from high brightness temperatures implied by the variations, brightness temperatures which are derived under the assumption of cosmological distances using standard Friedmann cosmology, nearly spherical source geometry, and nonrelativistic bulk motions. The brightness temperatures thus derived often greatly exceed the $\sim 10^{12}$ K limit imposed by self-Compton scattering if the radio emission is incoherent synchrotron radiation, the mechanism which almost certainly applies to the centimetric radio emission observed from the same sources (cf., Jones, O'Dell, and Stein 1974*a*, *b*; Burbidge, Jones, and O'Dell 1974).

Attempts to explain low-frequency variability by relaxing one of the above assumptions have not proven totally successful. Inherently high brightness temperature emission mechanisms (e.g., Petschek, Colgate, and Colvin 1976; Cocke, Pacholczyk, and Hopf 1978) should cause pronounced "fast" interstellar scintillation, which has not been observed (Condon and Dennison 1978). Relativistic beaming models with Lorentz factors as high as ~ 20 can reduce the brightness temperatures, but still often result in excessive energy requirements owing to the long radiative lifetimes of the synchrotron-emitting electrons (e.g., Blandford and McKee 1977). Most models in which the variability is extrinsic, caused by propagation effects (e.g., Shapirovskaya 1978; Marscher 1979), make predictions which have not been fulfilled.

Of these models, two are currently considered the leading contenders: the relativistic beaming model and the refractive scintillation model. The relativistic beaming model is considered attractive because it links phenomena observed at centimetric wavelengths (e.g., superluminal motion) with those found at longer wavelengths. Most sources have not been modeled in sufficient detail to determine how common the problem of energetics cited above is; even if the problem persists, nonspherical geometries (such as thin, planar shocks) can reduce it (Marscher 1982; O'Dell 1982). The refractive scintillation model, recently introduced by Rickett, Coles, and Bourois (1984), ascribes some or most low-frequency variability to "slow," refractive scintillations of the compact components in the sources by the interstellar medium in our

[1] NRAO is operated by Associated Universities, Inc., under contract with the National Science Foundation.

Galaxy. This model predicts a decrease in the level of variability with increasing frequency, as is observed in many sources (Spangler and Cotton 1981). (Above about 3 GHz, the variability typically becomes more pronounced but is probably not directly associated with variability at low frequencies.) Its main prediction is a decrease in the level of fluctuations with increasing angular size of a low-frequency component of a source.

The quasar NRAO 140 ($z = 1.258$) has properties which are particularly favorable for studying the cause of low-frequency variability. It exhibits $\sim$30% variability on time scales $\sim$1–2 yr at frequencies between 400 and 900 MHz (see, e.g., Altschuler *et al.* 1984). It is a superluminal source at centimeter wavelengths (Marscher and Broderick 1985). Finally, nearly all its emission at 18 and 6 cm arises from components with milliarc second (mas) sizes, thus allowing a definitive study of its structure using very long baseline interferometry (VLBI). Here we discuss the implications, with respect to the nature of low-frequency variability, of 18 cm VLBI observations of NRAO 140 at two epochs. Interpretation of the maps is aided by comparison with a 6 cm map obtained shortly after the second 18 cm experiment.

II. OBSERVATIONS AND MAPS

We observed NRAO 140 at 18 cm on 1984 April 4 using an eight element VLBI array with standard Mark II setup. The stations involved were the 100 m dish at Effelsberg (near Bonn), West Germany, operated by the Max-Planck-Institut für Radioastronomie (referred to as "BONN"); the 36 m antenna at Haystack Observatory near Westford, MA ("HSTK"); the 43 m antenna at the National Radio Astronomy Observatory, Green Bank, WV ("NRAO"); the 18 m antenna of the North Liberty Radio Observatory, operated by the University of Iowa ("IOWA"); the 26 m antenna at Harvard College Observatory, George R. Agassiz Station, Fort Davis, TX ("FDVS"); one of the 25 m antennas of NRAO'S Very Large Array near Socorro, NM ("VLA"); the 40 m antenna at the California Institute of Technology's Owens Valley Radio Observatory, Big Pine, CA ("OVRO"); and the 26 m antenna at the Hat Creek Radio Observatory, Hat Creek, CA, operated by the University of California ("HCRK"). In order to obtain a higher resolution map of the compact structure, we also observed the source at 6 cm on 1984 May 27, using a seven element VLBI array consisting of BONN, HSTK, NRAO, FDVS, VLA, OVRO, and HCRK. Again, a standard Mark II setup was employed. A receiver failure at HSTK limited the useful data to about 1.2 hr on baselines involving that antenna.

The data at both wavelengths were sufficient for maps with dynamic ranges in excess of 50:1 to be made. The correlation and much of the subsequent data reduction were performed at Caltech using the CIT-JPL Mark II correlator and the VLBI data reduction software developed by the Caltech and JPL staff, most notably T. J. Pearson. The remaining data analysis was completed using the same software on the Boston University Astronomy Computing Facility (VAX 11/750 and peripherals). During the mapping phase, the gains at each station (except BONN) were allowed to scale by a constant factor following S. Unwin's variation of the self-calibration procedure of Cornwall and Wilkinson (1981). A preliminary model fit was used in the initial mapping step at 6 cm, while the hybrid map model from 1981 October (Marscher and Broderick 1985) was used as the starting model at 18 cm. The latter procedure implies that any major differences between the 1981 October and 1984 April maps must be caused by differences in the data rather than by the choice of starting model.

The 18 cm and 6 cm hybrid maps are presented in Figures 1 and 2, respectively. Figure 2 gives the component nomenclature as adopted by Marscher and Broderick (1985). Component A has been shown to contain subcomponents when the source is observed at higher angular resolution at higher frequencies (Marscher and Broderick 1985; Marscher 1987). The 18 cm map contains two major sections, one to the northwest (hereafter designated "NW") containing the blended images of components A and B, and one to the southeast ("SE") containing the partially resolved combination of components C, D, and E. The map models are in exceptionally good agreement with the data, owing to the large number of stations in the arrays, the strength of the source, and the stability of the receivers, atmospheric transmission, and telescope pointing at 18 and 6 cm.

III. SITE OF THE 1981 LOW-FREQUENCY OUTBURST

Figure 3 presents both the 1981 October 18 cm map of Marscher and Broderick (1985) and the 1984 April map obtained by us. Close inspection reveals subtle differences between epochs in the sizes and levels of the contours of the maps. However, in light of the complex structure revealed at 6 cm (Fig. 2), it is difficult to interpret these differences solely through inspection of the maps. There are, nevertheless, two methods by which the differences can be analyzed more precisely. One is to form the ratio of the flux densities from each half of the source (excluding the weak extension to the southeast, which is poorly modeled in the 1981 October map). For our 1984 April map, the ratio of the flux density of NW to SE is 1.1, while the corresponding ratio for the 1981 October map is 0.86. It is therefore apparent that SE became fainter relative to NW between 1981 October and 1984 April. This is particularly interesting in light of the low-frequency light curve of NRAO 140 obtained by Altschuler *et al.* (1984). NRAO 140 underwent an outburst at frequencies less than $\sim$1 GHz, with a peak in flux density occurring near epoch 1981.6, very close to the epoch of the 18 cm map of 1981 October. The burst had subsided by the end of 1982, and the source remained at a lower flux density through mid-1984 (K. Mitchell, private communication). The outburst was evident at frequencies between 430 and 880 MHz. Since the amplitude of the outburst was $\sim$25% at 880 MHz, which is less than a factor of 2 different from 1660 MHz (the frequency of our 18 cm observations), the variable component would be required to have a precipitous high-frequency cutoff for it not to appear in our 18 cm maps. (The strongest falloff suggested is $\nu^{-2.2}$ in the slow scintillation model of Rickett, Coles, and Bourgois [1984]. Even this steep a frequency dependence would cause the variable component to contribute $\sim$0.15 Jy [$\sim$5%] more to the 1981 October map than to the 1984 April map.) We therefore conclude that the low-frequency variability should be evident in our 18 cm VLBI maps. The 18 cm flux density (as measured at BONN) dropped from 3.03 ± 0.05 Jy to 2.90 ± 0.05 Jy between the two epochs. This decrease (apparent also in Fig. 5 discussed below), combined with the increase in the ratio of NW to SE flux densities, leads us to conclude that the SE flux density decreased along with the decline at lower frequencies.

Determining which of the SE components was responsible

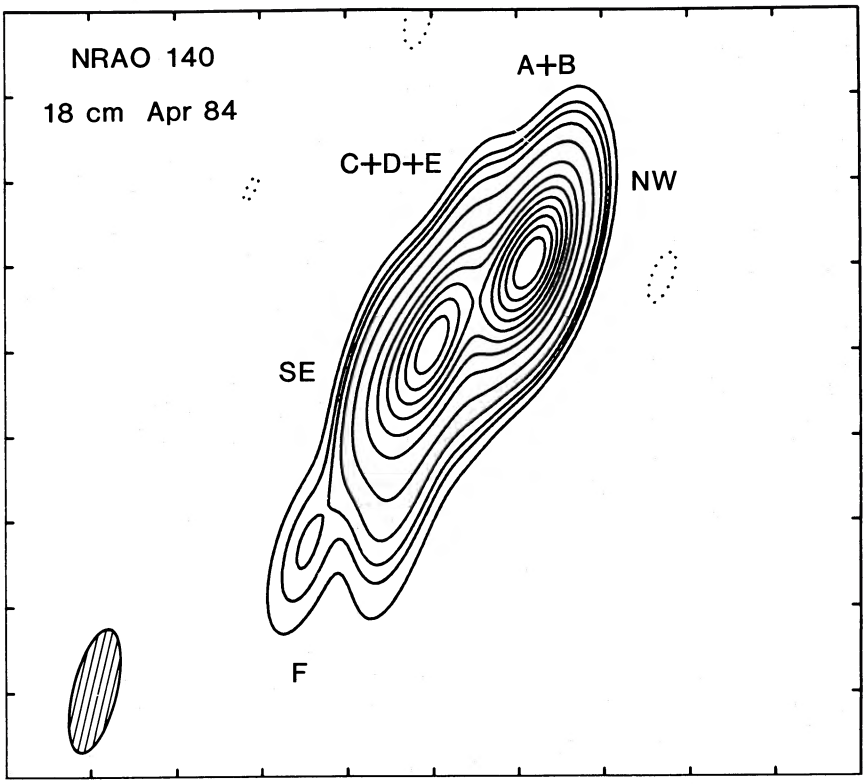

FIG. 1.—VLBI map of NRAO 140 at 18 cm, obtained in 1984 April. Contours are −0.5, 1, 2, 3, 5, 10, 20, ..., 90% of peak brightness temperature of 3.6×10^{10} K. Restoring beam is shown shaded in the lower left corner. North is up and east to the left. Tick marks are 4 mas apart. Blended combinations of components identified in Fig. 2 are marked. Designation "NW" refers to the half containing components A + B, while "SE" denotes the section containing C + D + E.

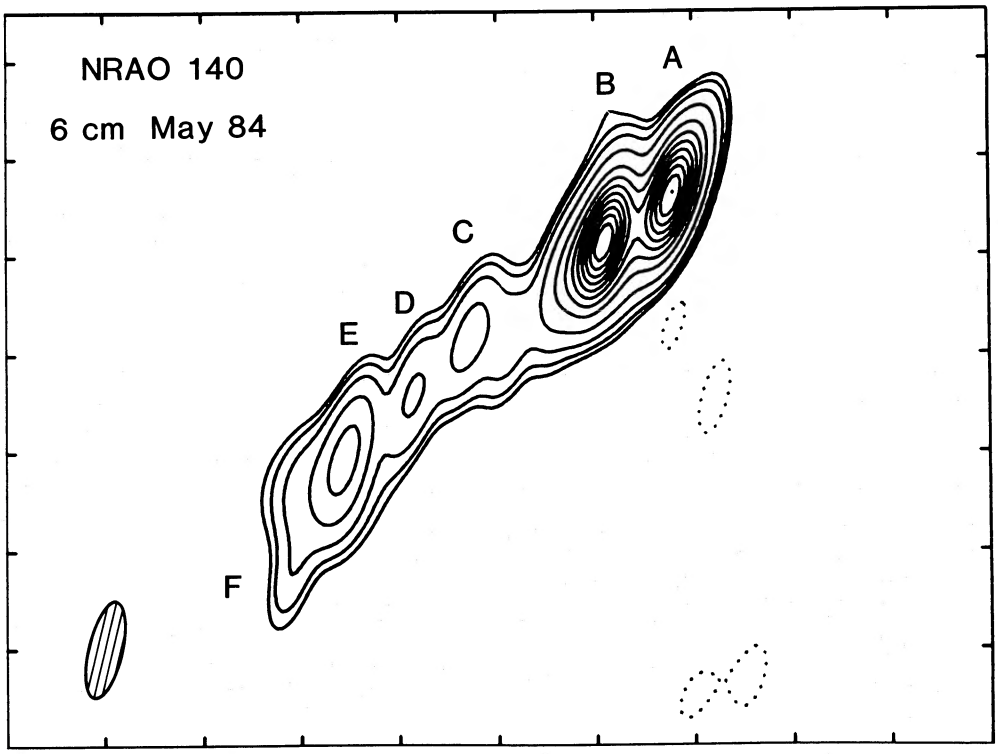

FIG. 2.—VLBI map of NRAO 140 at 6 cm, obtained in 1984 May. Contours are −1, 2, 3, 5, 10, 20, ..., 90% of peak brightness temperature of 2.3×10^{10} K. Restoring beam is shown shaded in the lower left corner. North is up and east to the left. Tick marks are 2 mas apart. Individual components referred to in the text are marked.

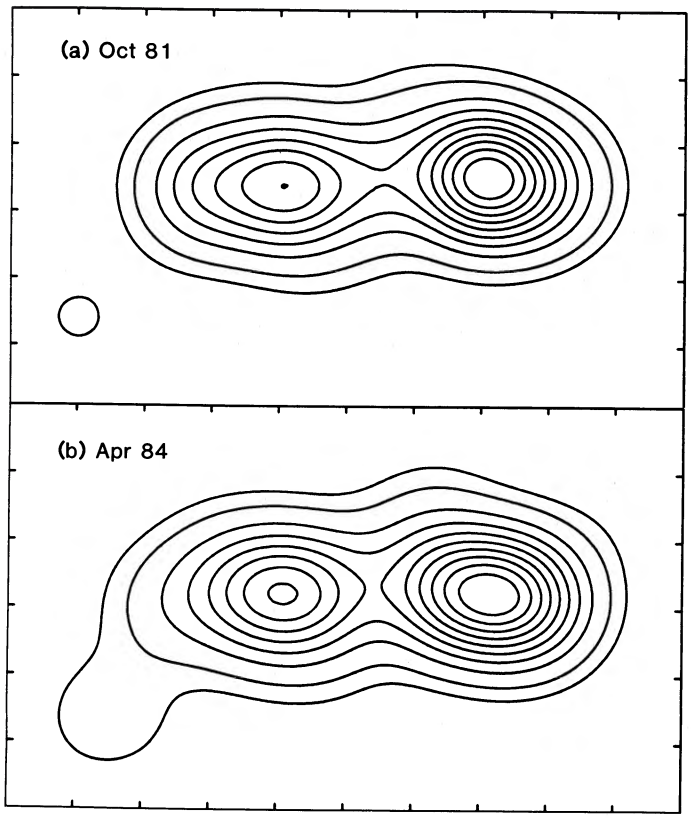

FIG. 3.—Two-epoch VLBI maps of NRAO 140 at 18 cm. Maps have been rotated clockwise by 40°. Restoring beam is a circular Gaussian with FWHM of 3.0 mas, which corresponds to the resolution along the position angle of the components. Contours are 5, 10, 20, ..., 90% of peak brightness temperature of 5.6×10^{10} K for 1981 October and 5.0×10^{10} K for 1984 April. Tick marks are 2 mas apart.

for the low-frequency event is not as straightforward. However, we are aided by changes in the visibility data between the two epochs. Comparison of visibility data can be more precise than comparison of maps since the latter can be affected by instabilities in the mapping procedure. Figure 4 shows a comparison between the 1981 October and 1984 April visibility data on selected baselines. Most obvious are changes in correlated flux density on the longest baselines, BONN–OVRO and BONN–HCRK, and in the associated closure phases. Of particular interest is the shift of the minimum in correlated flux density to a later GST. This shift in time corresponds to a shift in projected baseline toward shorter values. This property in turn corresponds to an increase in the separation of the brightness centroids of the SE and NW halves of the source. (This statement it is a slight oversimplification, since some of the structure is overresolved at these long baselines.) The increase in separation cannot be due to the superluminal expansion found by Marscher and Broderick (1985) in the NW half, since this would cause an apparent contraction between the NW and SE halves. We therefore interpret the shift in brightness centroid as being caused by either motion of the SE half away from the NW half, or shifts in the brightness distribution within the SE or NW half or both.

The BONN–OVRO baseline is 43.0 million wavelengths ($M\lambda$) in length and oriented along position angle (P.A.) 64°.7 (as projected onto the sky) at the visibility minimum of the 1981 October data. This translates to a baseline projected onto the jet axis of 18.2 $M\lambda$. The corresponding baseline at the visibility minimum of the 1984 April data is 41.8 $M\lambda$ along P.A. 64°.0, or 17.3 $M\lambda$ projected onto the jet axis. This shortening of the projected baseline of the minimum in correlated flux density is equivalent to an increase in separation of the NW and SE brightness centroids of 0.32 mas between the two epochs. (Again, this refers to the portion of the NW and SE components which are not overresolved on the BONN–OVRO baseline, and hence the apparent increase in separation can be caused by changes in the angular sizes or flux densities of the individual components or both.) If interpreted as an increase in actual separation, the separation rate between the two epochs would be 0.13 mas yr^{-1}. This is remarkably close to the (superluminal) separation rate of component B from the northwestern part of A (A1) of 0.15 ± 0.02 mas yr^{-1} (Marscher and Broderick 1985). Nevertheless, we regard this as a coincidence and instead favor the interpretation discussed below that the apparent separation is caused by changes in brightness of individual components of the source.

Further interpretation is aided by an analysis of the entire radio spectrum. Figure 5 shows the total radio spectrum of NRAO 140 at epochs 1981.7 and 1984.3, with the spectral decomposition suggested by multifrequency VLBI (this paper and Marscher 1987) obtained at the latter epoch. The flux densities of the individual components have been obtained via model fitting, with a starting model based on an inspection of the relevant hybrid map. While the decomposition into eight components is not well constrained solely by the VLBI and total flux measurements, we further constrain the fit by assuming that the noncore components (i.e., all components other than component A) behave as uniform, incoherent synchrotron sources with power-law optically thin spectra and spectral turnovers caused by self-absorption. The assumption of uniformity is probably the most questionable of these characteristics; inhomogeneities have the effect of broadening the spectral turnover. Even so, it is unlikely that our decomposition is grossly in error: the turnover frequencies of components B, C, and E cannot be adjusted by much without destroying the flatness of the spectrum between 0.4 and 2 GHz, even if inhomogeneities broaden the turnovers.

As can be seen from a comparison of the 1981.7 and 1984.3 spectra, the low-frequency variability was most pronounced between 408 and 880 MHz. This frequency range is coincident with the spectral peak of component C according to our decomposition. It is also possible for component E to peak in this spectral region, with component C turning over at a higher frequency, although the fit is poorer. However, if component E had declined in brightness between epochs 1981.7 and 1984.3, the brightness centroid of the SE component on the 18 cm maps would have moved toward the NW half rather than away from it. If, as our spectral decomposition suggests, component C was the site of the low-frequency event, the consequent decline in flux density on the northwestern end of the SE half between epochs 1981.7 and 1984.3 would lead naturally to the observed apparent shift of the brightness centroid to the southeast.

We therefore conclude that the VLBI data and radio spectrum together point to component C as the site of the 1981 low-frequency outburst in NRAO 140. This is the most precise specification of the site of low-frequency variability yet obtained for any source.

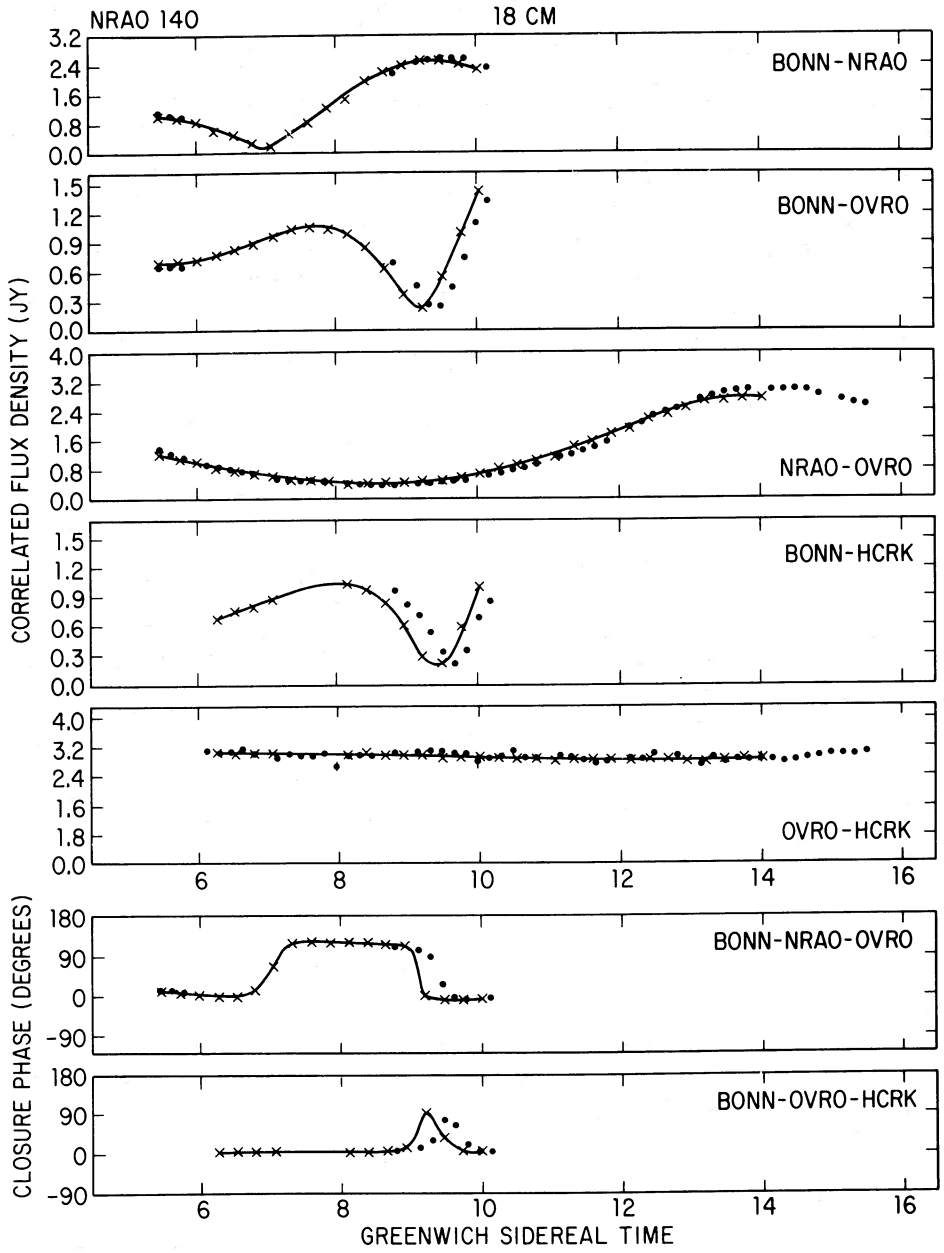

FIG. 4.—Visibility data of selected baselines for the 18 cm observations of 1984 April (*filled circles*) and 1981 October (denoted by symbol " × "). October 1981 data have been multiplied by 0.95 to compensate for difference in total flux density between epochs. *Solid curve:* hybrid map fitted to data of 1981 October. Of particular interest are the changes between epochs on the long BONN–OVRO and BONN–HCRK baselines.

IV. THE SELF-COMPTON PROBLEM RELATED TO LOW-FREQUENCY VARIABILITY IN NRAO 140

a) General Considerations

In the previous section, we identified component C of Figure 2 as the location of the low-frequency outburst which reached maximum brightness in 1981. This identification encourages us to compare the features of the competing models for low-frequency variability with the physical characteristics of this component and its variations in brightness.

The most prominent problem associated with low-frequency variability is the short time scale of the fluctuations, typically a few years (cf. Altschuler *et al.* 1984, and references therein). In the case of the 1981 low-frequency outburst in NRAO 140, the characteristic time scale of variability, as defined by Burbidge, Jones, and O'Dell (1974), is ~ 5 yr, which translates to an angular diameter $\lesssim 0.5\ h$ mas, where h is Hubble's constant in units of 100 km s^{-1} Mpc^{-1}, and $q_0 = 0$ has been assumed. The upper limit can be higher by a factor of 3 in the case of spherical geometry (see Burbidge, Jones, and O'Dell 1984). The brightness temperature of the source would then be $\sim 6 \times 10^{13}\ h^{-2}$ K at 0.5 GHz near the peak of the 1981 event. The above values are even more extreme if we assume that only component C varied. In this case, the component varied by over 60%, with a characteristic time scale ~ 2 yr, and angular diameter $\sim 0.2\ h$ mas, and a brightness temperature $\sim 2 \times 10^{14}\ h^{-2}$ K.

The angular size of component C cannot be measured at

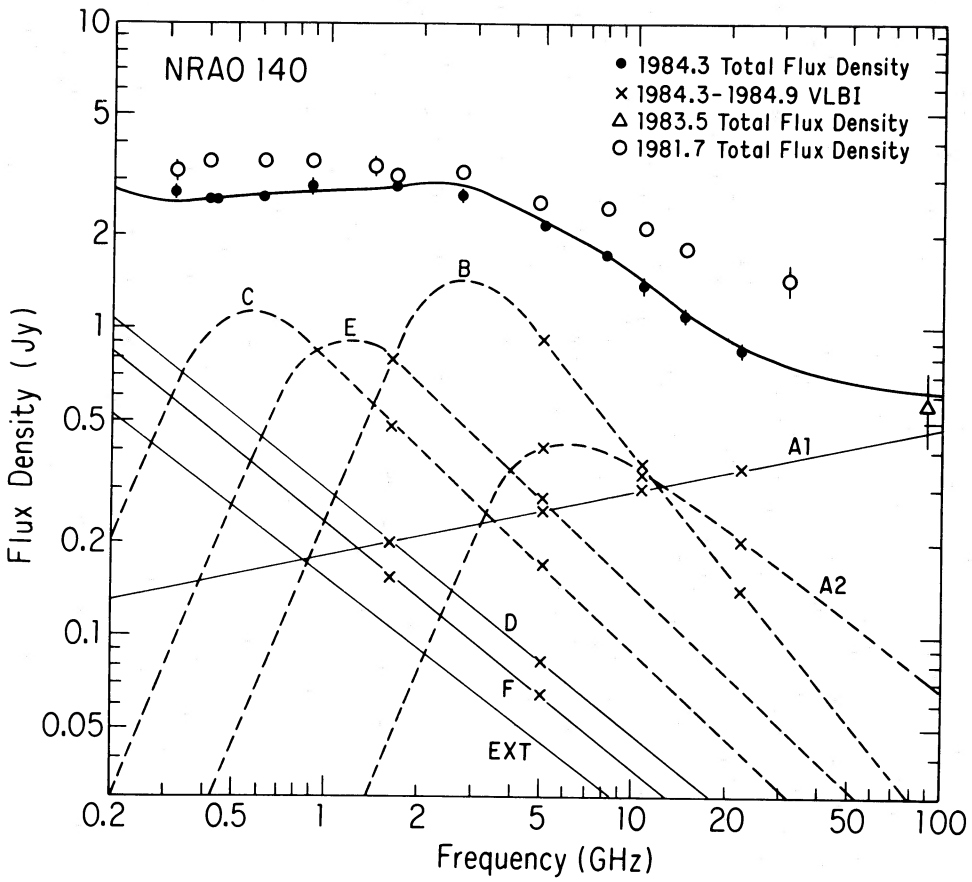

FIG. 5.—Radio spectrum of NRAAO 140. Total flux density is given for epochs 1981.7 and 1984.3. *Dashed curves*: spectra of individual components under the assumptions discussed in the text; and *solid curve*: the composite spectrum obtained by summing individual component contributions. VLBI data are from Marscher and Broderick (1985), Marscher (1987), and this work. Components B and E have the same flux density at 1.66 GHz. Spectrum of arcsecond-scale emission ("EXT") is taken from Schilizzi and de Bruyn (1983). Total flux density measurements are from Altschuler *et al.* (1984), Aller *et al.* (1985), Marscher and Broderick (1985), this work, H. and M. Aller (private communication), and W. Dent (private communication). Errors in total flux density are smaller than the symbols unless otherwise indicated. Errors in the individual component flux densities are typically ~10%, except for A1 at 1.66 GHz, A1 and A2 at 5 GHz, and all components at 22 GHz, for which the errors are ~20%.

18 cm because of insufficient angular resolution. At 6 cm, however, the east-west resolution of ~0.7 mas is adequate for measuring the dimensions of the component in directions not close to the P.A. of the long axis of the resolution beam, −15°. Both the hybrid map and model fitting yield a mean (=square root of major axis times minor axis) FWHM of 1.2 mas if the component is fitted with an elliptical Gaussian brightness distribution. Since the radiative transfer equations can be solved analytically if the source is assumed to be spherical, we translate the above value to an equivalent angular diameter of a spherical source, $\theta_s = 2.2$ mas. (This is obtained by multiplying the FWHM by 1.8 to yield the angular diameter of a spherical source which produces nearly the same visibility curve as the previously assumed Gaussian.) This value of the angular size implies a brightness temperature $\sim 2 \times 10^{12}\, h^{-2}$ K at 0.5 GHz. Although still about an order of magnitude above the self-Compton limit (in order for the self-Compton problem to be avoided, the brightness temperature must be *considerably* below $10^{12}[1+z]^{-1.2}$ K $= 4 \times 10^{11}$ K for NRAO 140), this value is not as extreme as that implied by the brightness variations. Furthermore, the steepness of the spectrum of component C above 1 GHz allows the possibility that the angular size is frequency dependent (caused, for example, by gradients in magnetic field strength and maximum electron energy). A frequency dependence as mild as $\theta \propto \nu^{-1/4}$ would reduce the maximum brightness temperature to $\sim 1 \times 10^{12}\, h^{-2}$ K, which, given the uncertainty in the analysis, could be within the self-Compton limit. Since the optically thin flux density is proportional to the emission coefficient times the effective volume of the source, this frequency dependence would yield the observed spectral index of −1 for an intrinsic spectral index (i.e., the spectral index of the emission coefficient) of −0.25 if the above frequency dependence applies also to the depth of the source along the line of sight, and −0.5 if the depth has no frequency dependence.

Hence, the conclusion that component C is the site of a low-frequency outburst in NRAO 140 does not present extreme theoretical difficulties when purely observed parameters are used. The self-Compton problem arises only when the time scale of variability is converted into an upper limit to the diameter, which in turn is translated into an angular size using the cosmological distance. The discrepancy between the measured angular size of component C at 6 cm and the angular size inferred from the brightness variations is a factor of $\sim 10\, h^{-1}$. Therefore, a much lower than assumed distance to NRAO 140 would solve the self-Compton problem associated

with the variability. We now consider several alternatives which have been proposed under the assumption that standard cosmological distances are in fact appropriate.

b) Nonspherical Geometries

The inference of a linear size from time scales of variability requires specification of the source geometry. Actually, the only length scale which has a direct connection to the variability time scale is the *dimension of the source along the line of sight*. Some authors (e.g., Marscher 1982, O'Dell 1982) have pointed out that emission regions which are compressed along the line of sight lead to variability times scales which can be significantly shorter than the commonly used transverse dimension divided by the speed of light. Such a geometry can arise, for example, if the radio emission originates behind a shock front (Marscher 1982; Aller and Aller 1982). In the case of NRAO 140, this would require a thickness along the line of sight $\sim 10\ h^{-1}$ times less than the transverse dimension. If the emission region is compressed along the axis of the jet, this further requires that the jet axis be aligned with the line of sight to within $\sim 5°$. This close an alignment has a likelihood of $\sim 0.4\%$ (if the jet is two-sided) unless favored by relativistic beaming. Thus, geometry alone cannot explain the low-frequency variability observed in a large fraction of sources (Condon *et al.* 1979; Dennison *et al.* 1981; Fanti *et al.* 1983; Gregorini, Ficarra, and Padrielli 1987), if the case of NRAO 140 is typical.

c) Relativistic Beaming

Relativistic beaming of the low-frequency radio emission can result in time contraction in the observer's frame, thereby leading to incorrect inference of linear sizes from time scales of variability (Rees 1967; Jones and Burbidge 1973; Burbidge, Jones, and O'Dell 1974). Furthermore, the self-Compton brightness temperature limit transforms as $\delta^{-1.2}$, where δ is the Doppler factor. The time scale of the low-frequency variability of NRAO 140 could be reconciled with the angular size measurement of component C at 6 cm if the Lorentz factor of the jet $\gtrsim 5$ and the jet points less than $\sim 10°$ away from the line of sight. This Lorentz factor could be reduced even further if a flattened geometry is allowed, and perhaps this could lower some of the uncomfortably high Lorentz factors needed to explain some sources. Relativistic beaming with Lorentz factor greater than ~ 5 in NRAO 140 can also explain the apparent superluminal motion observed at 2.8 cm (Marscher and Broderick 1985).

Two other problems connected with low-frequency variability are the excess self-Compton X-ray flux expected and the high total energy required (Jones and Burbidge 1973; Burbidge, Jones, and O'Dell 1974). These difficulties are also mitigated by relativistic beaming. We can use standard synchrotron formulas for a self-absorbed source (e.g., Marscher 1983; Marscher and Broderick 1985) to derive the self-Compton flux density and the total energy of component C. We adopt an angular diameter $\theta_s = 2.2$ mas (as obtained at 6 cm), a turnover frequency $\nu_m = 0.56$ GHz, optically thin flux density at ν_m (obtained by extrapolating the spectrum from higher frequencies) $S_m = 1.5$ Jy, upper frequency cutoff $\nu_2 \approx 50\nu_m$ (appears only in a logarithmic term in the formulas mentioned above), and a spectral index $\alpha = 1.0$ ($S_\nu \propto \nu^{-\alpha}$). Note that component C cannot have a turnover frequency much higher than about 0.6 GHz without destroying the flatness of the total spectrum at lower frequencies. These parameters yield a magnetic field $B \sim 1 \times 10^{-5}\delta$ gauss, self-Compton flux density $S_\nu^{sc}(E_{\rm keV}) \sim 3 \times 10^3 E_{\rm keV}^{-1}\delta^{-6}$ μJy (valid for $E_{\rm keV} \ll 400\delta^{-2}$), minimum required energy density in relativistic electrons $u_{re} \sim 6\ h\ \delta^{-5}$ ergs cm^{-3}, and total energy in relativistic electrons $E_{re} \sim 2 \times 10^{59}\ h^{-2}\ \delta^{-4}$ ergs, where it has been assumed that the Doppler factor is of the order of the Lorentz factor. A Doppler factor $\delta \sim 10$ then gives $B \sim 10^{-4}$ gauss, $S_\nu^{sc}(1\ {\rm KeV}) \sim 3 \times 10^{-3}$ μJy, and $E_{re} \sim 2 \times 10^{55}$ ergs. Even this high a Doppler factor results in the magnetic field being over two orders of magnitude below the equipartition value ($\delta \sim 50$ would be required for equipartition to hold). Component C lies a projected distance $\sim 30\ h^{-1}$ pc from the base of the jet. Hence, if the inclination of the jet axis to the line of sight $\sim \sin^{-1}(1/\delta) \sim 0.1$ radians, the actual distance $\sim 300\ h^{-1}$ pc $\sim 10^3$ lt-yr. Component C is then more than $\sim 10^3$ yr old; hence, the energy input rate averaged over the lifetime of component C need not exceed 10^{45} ergs s^{-1}. Since there are several major components in NRAO 140, a total energy input rate several times this value is required to maintain the radio source at its present level of activity. This energy requirement is quite modest in light of the much higher X-ray luminosity ($\gtrsim 10^{47}$ ergs s^{-1}; see Marscher 1987).

We therefore find that a relativistic jet model, with parameters similar to those required to explain the properties of the source at higher frequencies (cf. Marscher and Broderick 1985), solves the low-frequency variability problems of NRAO 140 with reasonable energetics.

d) Refractive Scintillation

An attractive alternative to the above model is to assume that the variability at low frequencies is caused by propagation effects (e.g., Shapirovskaya 1978). Rickett, Coles, and Bourgois (1984) have proposed that a large fraction of the flux variations observed at low frequencies could arise from refractive ("slow") scintillation of the radio waves as they encounter electron density irregularities in the local interstellar medium. Such scintillation would occur only in compact sources. Hence, the same population of sources from which superluminals and optically violent variables are commonly found would be expected to vary at low frequencies on time scales of a few years.

According to Rickett, Coles, and Bourgois (1984), the interstellar electron density irregularities scatter the radio waves into a solid angle of diameter $\theta_{\rm scat} \propto \nu^{-2.2}$. A source of intrinsic (Gaussian FWHM) angular diameter θ_i would have fractional variability of roughly unity for $\theta_i < \theta_{\rm scat}$ and $\sim 1.4(\theta_{\rm scat}/\theta_i)$ for $\theta_i \gtrsim 1.4\theta_{\rm scat}$, with a characteristic time scale

$$t_{\rm var} \approx 12 L_{\rm kpc}\, v_{100}{}^{-1}(\theta_i{}^2 + \theta_{\rm scat}{}^2)^{1/2} \text{ days}\,, \qquad (1)$$

where angular diameters are measured in mas, $L_{\rm kpc}$ is the distance to the scattering "screen" in kiloparsecs, and v_{100} is the velocity of the screen in units of 100 km s^{-1}. The scattering diameter of NRAO 140 at 1 GHz $\sim$ 1–2 mas (from Fig. 1 of Cordes, Ananthakrishnan, and Dennison [1984] using NRAO 140's galactic latitude $b = 19°$). If we adopt the 6 cm Gaussian FWHM of component C, we have $\theta_i \sim 1.2$ mas and $\theta_{\rm scat}(1\ {\rm GHz}) \sim 1.5 \pm 0.5$ mas. We then expect $\sim 100\%$ variability on a time scale $t_{\rm var} \sim 20 L_{\rm kpc}\, v_{100}{}^{-1}$ days at 1 GHz and $t_{\rm var} \sim 4\ L_{\rm kpc}\, v_{100}{}^{-1}$ months at 0.4 GHz. We expect that $L_{\rm kpc} \approx 0.5$ cosec $b \approx 1.5$ and $v_{100} \sim 0.1$ to 1. Using these values, we obtain $t_{\rm var} \sim 30$ to 300 days at 1 GHz and $t_{\rm var} \sim 0.6$ to 6 yr at 0.4 GHz. These values compare well with the observed time scale of a few years.

Although refractive scintillation solves the traditional problems of low-frequency variability associated with conversion of time scales to angular diameters, it does not affect the severity of the energetic requirements calculated above. In the absence of relativistic beaming, the total energy in relativistic electrons in component C is $\sim 2 \times 10^{59} x^{-6} h^{-2}$ ergs, where x is the ratio of the angular size at the turnover frequency, $\nu_m \approx 0.56$ GHz, to that at 5 GHz measured using our VLBI observations. For this to be reduced by ~ 4 orders of magnitude to a more "reasonable" value, the angular size would have to depend strongly on frequency, at least as $\theta \propto \nu^{-0.7}$. In order for component C to have a spectral index of -1.0, the intrinsic spectrum would have to rise as $\nu^{0.4}$, marginally steeper than the maximum dependence ($\propto \nu^{1/3}$) allowed. (In addition, this limit is reached only for a source with a lower energy cutoff to its electron energy distribution; such a source would not have an angular size which depends inversely on frequency.) Furthermore, it is not possible for synchrotron self-absorption opacity effects to yield a negative spectral slope. The strongest "reasonable" frequency dependence would be $\theta \propto \nu^{-1/2}$. This would yield an energy content exceeding $\sim 3 \times 10^{56}$ ergs and would imply a flat emission-coefficient spectrum. Although this solution is not beyond belief, it is far from satisfactory since such flat intrinsic spectra are not commonly observed in optically thin sources.

Thus the slow scintillation model requires an additional feature such as relativistic motion to lower the required energy content to an acceptable value.

e) High Brightness Temperature Emission Mechanisms

If the radiation at low frequencies is not standard, incoherent synchrotron emission, the brightness temperature limit and calculation of the energy requirements are invalid. Our observations do not directly test these models (some of which are cited in § I). However, it is difficult to construct a high brightness temperature model which reproduces the lumpy jet geometry (see Fig. 2) without also predicting a much higher degree of circular polarization than is observed (typically less than $\sim 1\%$; Weiler and de Pater 1983). Also, component C is not far from the self-Compton limit; this would be entirely fortuitous if not caused by Compton cooling in the context of standard, incoherent synchrotron theory.

V. SUMMARY

We have use VLBI and spectral observations to identify the specific site of a low-frequency outburst in NRAO 140. The component is quite compact at 6 cm; spectral considerations do not allow the angular size to have a strong frequency dependence. The *observed* brightness temperature of the component is not in gross conflict with the self-Compton limit, but the energy requirements are severe in the absence of mitigating effects such as noncosmological redshifts, relativistic beaming, or a "nonstandard" emission mechanism. If refractive scintillation causes the variability, it must operate in the presence of at least one such effect.

If refractive scintillation is the underlying mechanism by which the source varies at low frequencies, the variations should have lower amplitudes and shorter time scales at higher frequencies. Expression (1) implies that component C should vary by $\sim 40\%$ on a time scale $t_{\rm var} \sim 23$ to 230 days at 18 cm. Such "flickering" at 18 cm should be easily detectable using VLBI techniques. If component C is moving relativistically, its apparent superluminal motion should be detectable at 6 cm in a few years.

Since refractive scintillation is apparently observed in pulsars (Sieber 1982; Rickett, Coles, and Bourgois 1984), it would be surprising if it did not operate at some level in low-frequency variables. Since relativistic motion appears to be required to explain apparent superluminal motion in some of the same sources, it would not be surprising if both effects occur simultaneously.

The authors thank the staff at the observatories for their diligent assistance during our VLBI experiments. They also thank the staff at Caltech, especially S. Unwin and G. Dvorak, for their assistance during the correlation process. H. and M. Aller, K. Mitchell, and W. Dent kindly supplied us with unpublished total flux density measurements. We appreciate helpful discussions with B. Rickett. VLBI at Haystack Observatory, Harvard College Observatory, North Liberty Radio Observatory, Owens Valley Radio Observatory, and Hat Creek Radio Observatory are partially funded through the National Science Foundation. A. P. M. was funded in part by NSF grants AST-8315556 and AST-8516548.

REFERENCES

Aller, H. D., and Aller, M. F. 1982, in *Low-Frequency Variability of Extragalectic Radio Sources*, ed. W. D. Cotton and S. R. Spangler (Green Bank: National Radio Astronomy Observatory), p. 105.
Aller, H. D., Aller, M. F., Latimer, G. E., and Hodge, P. E. 1985, *Ap. J. Suppl.*, **59**, 513.
Altschuler, D. R., Broderick, J. J., Condon, J. J., Dennison, B., Mitchell, K. J., O'Dell, S. L., and Payne, H. E. 1984, *A.J.*, **89**, 1784.
Blandford, R. D., and McKee, C. F. 1977, *M.N.R.A.S.*, **180**, 343.
Burbidge, G. R., Jones, T. W., and O'Dell, S. L. 1974, *Ap. J.*, **193**, 43.
Cocke, W. J., Pacholczyk, A. G., and Hopf, F. A. 1978, *Ap. J.*, **226**, 26.
Condon, J. J., and Dennison, B. 1978, *Ap. J.*, **224**, 835.
Condon, J. J., Ledden, J. E., O'Dell, S. L., and Dennison, B. K. 1979, *A.J.*, **84**, 1.
Cordes, J. M., Ananthakrishnan, S., and Dennison, B. 1984, *Nature*, **309**, 689.
Cornwell, T. J., and Wilkinson, P. J. 1981, *M.N.R.A.S.*, **196**, 1067.
Cotton, W. D., and Spangler, S. R., eds. 1982, *Low-Frequency Variability of Extragalactic Radio Sources* (Green Bank: National Radio Astronomy Observatory).
Dennison, B., Broderick, J. J., Ledden, J. E., O'Dell, S. L., and Condon, J. J. 1981, *A.J.*, **86**, 1604.
Fanti, C., Fanti, R., Ficarra, A., Gregorini, L., Mantovani, F., and Padrielli, L. 1983, *Astr. Ap.*, **118**, 171.
Gregorini, L., Ficarra, A., and Padrielli, L. 1987, *Astr. Ap.*, submitted.
Hunstead, R. W. 1972, *Ap. Letters*, **12**, 193.
Jones, T. W., and Burbidge, G. R. 1973, *Ap. J.*, **186**, 791.
Jones, T. W., O'Dell, S. L., and Stein, W. A. 1974*a*, *Ap. J.*, **188**, 353.
———. 1974*b*, *Ap. J.*, **192**, 259.
Marscher, A. P. 1979, *Ap. J.*, **228**, 27.
———. 1982, in *Low-Frequency Variability of Extragalactic Radio Sources*, ed. W. D. Cotton and S. R. Spangler (Green Bank: National Radio Astronomy Observatory), p. 83.
———. 1983, *Ap. J.*, **264**, 296.
———. 1987, *Ap. J.*, submitted.
Marscher, A. P., and Broderick, J. J. 1985, *Ap. J.*, **290**, 735.
O'Dell, S. L. 1982, in *Low-Frequency Variability of Extragalactic Radio Sources*, ed. W. D. Cotton and S. R. Spangler (Green Bank: National Radio Astronomy Observatory), p. 89.
Petschek, A. G., Colgate, S. A., and Colvin, J. D. 1976, *Ap. J.*, **209**, 356.
Rees, M. J. 1967, *M.N.R.A.S.*, **135**, 345.

Rickett, B. J., Coles, W. A., and Bourgois, G. 1984, *Astr. Ap.*, **134**, 390.
Schilizzi, R. T., and de Bruyn, A. G. 1983, *Nature*, **303**, 26.
Shapirovskaya, N. Ya. 1978, *Sov. Astron. AJ*, **22**, 544.
Sieber, W. 1982, *Astr. Ap.*, **113**, 311.
Spangler, S. R., and Cotton, W. D. 1981, *A.J.*, **86**, 730.
Weiler, K. W., and de Pater, I. 1983, *Ap. J. Suppl.*, **52**, 293.

NORBERT BARTEL: Harvard-Smithsonian Center for Astrophysics, 60 Garden Street, Cambridge, MA 02138
JOHN J. BRODERICK: Department of Physics, Virginia Polytechnic and State University, Blacksburg, VA 24061
ALAN P. MARSCHER: Department of Astronomy, Boston University, 725 Commonwealth Ave., Boston, MA 02215
LUCIA PADRIELLI: Instituto di Radioastronomia, Via Irnerio 46, I-40126 Bologna, Italy
JONATHAN D. ROMNEY: National Radio Astronomy Observatory, Edgemont Road, Charlottesville, VA 22903-2475